Conducting Polymers Based on Alkylthiopyrroles

Hongchao Li, Christoph Lambert,* and Rainer Stahl

Institut für Organische Chemie, Bayerische Julius-Maximilians-Universität Würzburg, Am Hubland, D-97074 Würzburg, Germany

Received January 25, 2006

ABSTRACT: Three 3,4-bis(alkylthio)pyrroles (**5a**−**c**) were synthesized by a nonclassical pyrrole ring formation reaction followed by alkylation of the dithiol-2-one functional group. UV−vis absorption studies together with time dependent density-functional theory (TD-DFT) computations suggest that the monomers (**5a**−**c**) display low-energy $\pi-\sigma^*$ transitions (**5a**, 254 nm; **5b**, 232 nm; **5c**, 240 nm) compared to pyrrole (208 nm). Cyclic voltammetry investigations show that the monomers **5a**−**c** possess significantly lower oxidation potentials (0.60 V for **5a**, 0.58 V for **5b**, and 0.71 V for **5c**) than unsubstituted pyrrole (1.0 V). The corresponding polymers were successfully prepared by anodic electropolymerization and/or chemical oxidation ($FeCl_3$ as oxidant) and investigated by cyclic voltammetry, spectroelectrochemistry and in situ conductivity studies. Our investigations of monomeric 3,4-disubstituted pyrroles and corresponding polymers suggest that the electron donating alkylthio substituents at the 3- and 4-positions of the pyrrole ring play an important role for the electrochemical properties of polymers; e.g., the maximal conductivity of poly(ethylenedithiopyrrole) is ca. 10 times higher than that of poly[bis(propylthio)-pyrrole].

Introduction

Pyrrole and its derivatives, particularly 3,4-disubstituted 1*H*-pyrroles,[1] are important synthetic targets as versatile building blocks for bioactive molecules such as porphyrins,[2] alkaloids,[3] and co-enzymes,[4] and more recently for functional polypyrroles.[5−8] As far as conducting polypyrroles are concerned, not only do substituents at the 3- and 4-positions of pyrrole prevent the undesirable α-β coupling which decreases the effective conjugation length and the solubility of polypyrroles but also the substitution plays an important role for the electrical and electrooptical properties of the polymers.[9] However, the steric effect of such β-substitution should not be ignored. For example, poly(3,4-dimethylpyrrole) possesses a lower conjugation length and a lower electrical conductivity than poly(pyrrole) itself.[10] Simultaneously, substitutions also affect the electronic states of pyrrole and that of corresponding polypyrroles. Consequently, the introduction of electron donating substituents at the β positions of pyrrole might be an interesting strategy to prevent defects and withhold or even surpass the desirable electrooptical properties of polypyrrole. Unfortunately, the synthesis of such 3,4-disubstituted pyrroles remains a challenge for synthetic chemists since the 2- and 5-positions of electron-rich pyrrole possess the well-known higher reactivity.[11]

Until now, only a few multistep methods for the synthesis of 3,4-disubstituted pyrroles have been reported. On the basis of a coupling reaction of imines and nitroalkanes catalyzed by a lanthanide complex, 3,4-alkylpyrroles were synthesized in reasonable yields.[12] Wong et al. reported the preparation of a 3,4-disubstituted pyrrole starting from a 3,4-bis(trimethylsilyl)-1*H*-pyrrole.[13] By cyclocondensation of aryl styryl sulfones and benzyl styryl sulfones with tosyl methyl isocyanide, 3,4-disubstituted pyrroles were obtained.[14] 3,4-Disubstituted pyrroles were also synthesized via a tosylmethyl isocyanide (TosMIC) based route.[15] Bromination of 1-[tri(1-methylethyl)silyl]pyrrole and the following halogen−metal exchange chemistry can afford 3,4-disubstituted pyrroles.[16] The syntheses of 3,4-disubstituted pyrroles have also been reported via Diels−Alder reaction.[17] However, most of the known synthetic routes are often complicated and limited to some substituent families.

Scheme 1. Chemical Structures of EDOT, Edtt and EDOPy

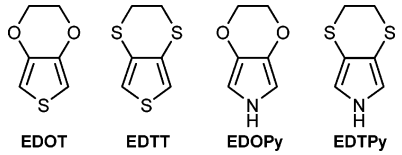

On the other hand, heterocycle-based conjugated polymers such as polythiophenes (PThs) and polypyrroles (PPys) have attracted significant attention due to the promising applications for light-emitting diodes,[18] electrochromic devices,[19] field-effect transistors,[20] and plastic photovoltaic devices.[21] Since the first report on the novel conducting polymer poly(3,4-ethylenedioxythiophene) (PEDOT), 3,4-ethylenedioxythiophene (EDOT) (Scheme 1) and its derivatives have intensely been studied as building blocks for the design of various classes of molecular π-conjugated systems with interesting electronic and optical properties.[22] As a direct analogue of the well-known EDOT, ethylenedithiothiophene (EDTT)[23,31] was recently investigated because of its specific properties related with the sulfur atoms, such as potential S···S interactions.[24] The synthesis and properties of ethylenedioxypyrrole (EDOPy) was also reported.[25] The low oxidation potential of EDOPy is expected to promote the low potential oxidation polymerization. More recently, we worked out the synthesis of a 3,4-disubstituted pyrrole **5a** with an electron donating methylenedithio bridge and investigated its application as a monomer for electroactive polymers.[26] To take a further step, ethylenedithiopyrrole (EDTPy, **5b**) and its analogues are highly decisive building blocks to develop new functional heterocycle-based conjugated polymers and to manipulate the physicochemical, electronic and optical properties of such systems. In this paper, we will report in detail on the new synthesis of 3,4-disubstituted pyrroles **5a**, **5b**, and **5c** with electron donating alkylthio groups and on the studies of the corresponding conducting polymers.

* Corresponding author: Fax: +49 931 8884606. Telephone: +49 931 8885318. E-mail: lambert@chemie.uni-wuerzburg.de.

10.1021/ma0601868 CCC: $33.50
Published on Web 02/24/2006

Experimental Section

General Data. UV−vis−NIR absorption spectra were recorded with a Jasco V-750 spectrometer. All electrochemical investigations were carried out with a computer controlled BAS CV50W potentiostat in dried and oxygen-free acetonitrile (CH_3CN, ACN) using 0.1 M tetrabutylammonium hexafluorophosphate (TBAH) as supporting electrolyte, platinum disk (Pt) as working electrode, platinum wire as counter and a Ag/AgCl reference electrode. The redox potentials were referenced against internal ferrocene/ferrocenium (Fc/Fc^+). The spectroelectrochemical measurements were performed in reflection mode using a polished platinum disk working electrode with a Jasco V-750 spectrometer in an electrochemical three-electrode cell controlled by EG&E model 363 potentiostat. The in situ conductivity measurements were carried out using two-band working electrodes (Pt, interband spacing is 20 μm) bridged by the deposited polymers according to the reported procedure.[27] The lead resistance was neglected. For each measurement, the anodic polymer deposition was stopped until minimum resistance was obtained, that is, the conductance becomes independent of the film thickness.

All chemical reactions were carried out under an atmosphere of dry N_2 unless otherwise stated. DMF and ACN were distilled from CaH_2. MeOH was distilled from sodium methoxide. Sodium tosylamide (TsNHNa) was prepared by reaction of *p*-toluenesulfonamide with a mixture of sodium ethoxide in ethanol under reflux. 4,5-Bis(bromomethyl)-1,3-dithiole-2-thione (**1**) was synthesized according to the reported procedure.[28] All other reagents were standard grade and used as received.

4,6-Dihydro-*N*-tosyl-(1,3)-dithiolo[4,5-*c*]pyrrol-2-thione (2). To a suspension of sodium tosylamide (4.0 g, 20.7 mmol) in anhydrous acetonitrile (100 mL) at 80 °Cwas added a solution of **1** (3.2 g, 10.0 mmol) in anhydrous DMF (10 mL) dropwise over a period of 20 min. The resulting brown reaction mixture was stirred for another 1 h before filtration through Celite column (1 cm). The filter was washed with DMF, and the combined filtrates were poured into water to give brown precipitates which were collected by filtration and washed with acetonitrile. After drying in a vacuum, 2.8 g of brownish yellow solid was obtained in a yield of 85%. ^{1}H NMR (DMSO-d_6), δ/ppm: 7.74 (2H, d, J = 8.3 Hz, Ar−H), 7.46 (2H, d, J = 8.3 Hz, Ar−H), 4.47 (4H, s, $-CCH_2-N$), 2.40 (3H, s, $Ar-CH_3$).

***N*-Tosyl-(1,3)-dithiolo[4,5-*c*]pyrrol-2-thione (3).** A mixture of **2** (0.33 g, 1.0 mmol) and 2.5 equiv of 2,3-dichloro-5,6-dicyano-1,4-benzoquinone (DDQ) in chlorobenzene (20 mL) was refluxed for 12 h. After removal of the solvent in a vacuum, the brown residue was purified by chromatography on a silica gel column using CH_2Cl_2/petroleum ether (PE) as eluent. So, 0.25 g of yellow solid was obtained in a yield of 75%. ^{1}H NMR ($CDCl_3$), δ/ppm: 7.80 (2H, d, J = 8.4 Hz, Ar−H), 7.36 (2H, d, J = 8.4 Hz, Ar−H), 7.16 (2H, s, Py−H), 2.45 (3H, s, $Ar-CH_3$).

***N*-Tosyl-(1,3)-dithiolo[4,5-*c*]pyrrol-2-one (4).** Mercuric acetate (1.1 g, 3.6 mmol) was added in one portion to a suspension of **3** (5.88 g, 1.8 mmol) in a mixture of $CHCl_3$ (30 mL) and glacial acetic acid (3 mL) causing the initially yellow solution to turn into white. The resulting reaction mixture was stirred for 4 h at room temperature. The white precipitates were filtered through a Celite column (1.0 cm) and washed thoroughly with CH_2Cl_2. The combined organic phase was washed with saturated aqueous $NaHCO_3$ solution, water and then dried over anhydrous $MgSO_4$. Removal of solvents afforded a colorless solid with a yield of 98%. ^{1}H NMR ($CDCl_3$), δ/ppm: 7.78 (2H, d, J = 8.4 Hz, Ar−H), 7.34 (2H, d, J = 8.4 Hz, Ar−H), 7.22 (2H, s, Py−H), 2.44 (3H, s, $Ar-CH_3$).

3,4-Methylenedithiopyrrole (5a). *N*-Tosyl-(1,3)-dithiolo[4,5-*c*]-pyrrol-2-one (0.15 g, 0.5 mmol) was dissolved in 16 mL of anhydrous THF−MeOH (1:1 v/v) and degassed (N_2, 30 min) before the addition of sodium methoxide (5 M in MeOH, 10 mmol). The yellow solution was refluxed for 60 min and cooled; 1 mL of dichloromethane was added to the resulting orange reaction mixture. The mixture was stirred at room temperature for further 60 min. The reaction was stopped by addition of H_2O (100 mL) and extracted with dichloromethane. The combined organic phase was washed with H_2O and dried over anhydrous $MgSO_4$. After concentration in a vacuum, the crude product was purified by column chromatography (silica gel, CH_2Cl_2/PE, 1:2) to give 0.096 g of a colorless solid product in 65% yield. ^{1}H NMR ($CDCl_3$), δ/ppm: 7.65 (2 H, d, J = 8.4 Hz, Ar−H), 7.24 (2H, d, J = 8.4 Hz, Ar−H), 6.78 (2H, s, Py−H), 4.60 (2H, s, $-SCH_2S-$), 2.35 (3H, s, $Ar-CH_3$). MS (EI): m/z 297 (M^+, 100%), 142 (M^+-Ts, 77%). The obtained *N*-tosyl-3,4-methylenedithiopyrrole (0.32 mmol) was refluxed in MeOH−THF (10 mL, 1/1 v/v) in the presence of MeONa (6.4 mmol) for another 60 min before addition of H_2O, and the pH of the reaction mixture was adjusted to pH = 7 by addition of 4 M aqueous HCl solution. The mixture was extracted with CH_2Cl_2, and the combined organic phase was dried over anhydrous $MgSO_4$. After concentration in a vacuum, the crude product was purified by column chromatography (silica gel, CH_2Cl_2/PE, 1:1) to give 0.039 g (yield 85%) of 3,4-methylenedithiopyrrole as colorless crystals. ^{1}H NMR (acetone-d_6), δ/ppm: 9.62 (1H, b, NH), 6.38 (2H, s, Py−H), 4.52 (2H, s, $-SCH_2S-$). ^{13}C NMR (acetone-d_6), δ/ppm: 124.9, 113.8, 48.7. MS (EI): m/z 143 (M^+, 100%).

3,4-Ethylenedithio-pyrrole (5b). A suspension of **4** (0.15 g, 0.5 mmol) in anhydrous MeOH (10 mL) was degassed by N_2 before addition of sodium methoxide (2 mL of 5 M in MeOH). The reaction mixture was stirred at room temperature for 1 h to give a yellow solution. Then 0.05 mL of dibromoethane was added in one portion, and the reaction mixture was stirred for 24 h. The resulted suspension was treated with aqueous HCl solution (0.5 M) and extracted with dichloromethane. After removal of solvents, the residue was purified by chromatography on silica gel using CH_2Cl_2/PE (3/2) as eluent to afford a colorless solid in a yield of 77%. ^{1}H NMR (acetone-d_6), δ/ppm: 9.90 (1H, b, NH), 6.47 (2H, s, Py−H), 3.01 (4H, s, $-SCH_2CH_2S-$). ^{13}C NMR (acetone-d_6), δ/ppm: 117.46, 109.75, 30.59. MS (EI): m/z 157 (M^+, 100%).

3,4-Bis(propylthio)pyrrole (5c). A suspension of **4** (0.15 g, 0.5 mmol) in anhydrous MeOH (10 mL) was degassed by N_2 before addition of sodium methoxide (2 mL of 5 M in MeOH). The reaction mixture was stirred at room temperature for 1 h to give a yellow solution. Then, 0.15 mL of C_3H_7Br (1.5 mmol) was added in one portion, and the mixture was stirred for 24 h. The resulted suspension was treated with aqueous HCl solution (0.5 M) and extracted with dichloromethane. After removal of solvents, the residue was purified by chromatography on silica gel using CH_2Cl_2/PE (3/2) as eluent to afford an oil which turned into a colorless solid after drying in a vacuum in a yield of 55%. ^{1}H NMR (acetone-d_6), δ/ppm: 10.10 (1H, b, NH), 6.74 (2H, s, Py−H), 2.51 (4H, t, J = 7.2 Hz, $-SCH_2-$), 1.38 (4H, m, J = 7.4 Hz, $-SCCH_2-$), 0.80 (6H, t, J = 7.4 Hz, $-CH_3$). ^{13}C NMR (acetone-d_6), δ/ppm: 126.11, 118.43, 40.61, 25.30, 15.53. MS (EI): m/z 215 (M^+, 42%), 131 ($M^+ - 2C_3H_6$, 100%).

Poly(3,4-Methylenedithiopyrrole) (Poly(5a)). 5a (72 mg, 0,5 mmol) was dissolved into 5 mL of acetonitrile and stirred. A solution of $FeCl_3$ (5 mL of 0.1 M in acetonitrile) was added in one portion to the stirred solution of **5a** to give a purplish black mixture. The resulted purplish black precipitates were collected after stirring for further 3 h and washed with water and acetone, respectively. After being dried in a vacuum, poly(**5a**) was obtained as purplish black powder.

Results and Discussion

Synthesis. The syntheses of 3,4-disubstituted pyrroles (**5a**−**c**) is outlined in Scheme 2. The starting material 4,5-bis-(bromomethyl)-1,3-dithiol-2-thione (**1**) was synthesized according to the reported procedure.[28] The formation of pyrrole ring was achieved via a nonclassical pyrrole synthesis.[28] Cyclization reaction of **1** with 2 equiv of sodium tosylamide afforded the dihydropyrrolo compound **2** in about 90% yield. Dehydrogenation of **2** using 2 equiv of DDQ in chlorobenzene gave the *N*-tosyl-(1,3)-dithiolo[4,5-*c*]pyrrol-2-thione (**3**), and *N*-tosyl-

Scheme 2. Synthesis of Monomers[a]

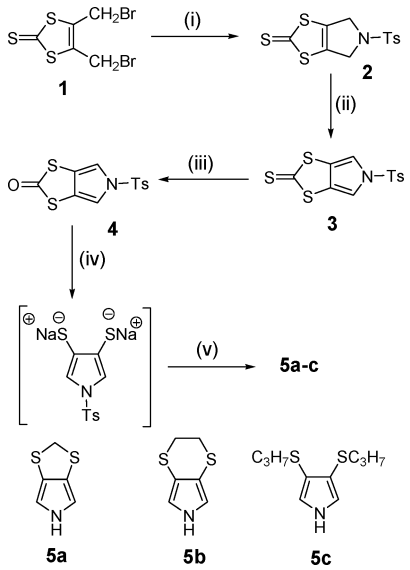

[a] Reagents and conditions: (i) TsNHNa, MeCN-DMF, 80 °C, 2 h; (ii) DDQ, PhCl, reflux, 4 h; (iii) $Hg(OAc)_2$, $CHCl_3$−AcOH, room temperature, 4 h; (iv) NaOMe, MeOH, room temperature, 1 h; (v) RX (CH_2Cl_2 for **5a**; $BrCH_2CH_2Br$ for **5b**; C_3H_7Br for **5c**); NaOMe, room temperature, 3 h.

(1,3)-dithiolo[4,5-*c*]pyrrol-2-one (**4**) was obtained via a transchalcogenation reaction with mercuric acetate in a mixture of chloroform and glacial acetic acid. It has been reported that alkylation of the dithiolone compounds can be accomplished by treatment with excess of sodium methoxide followed by reaction with alkylhalogen.[29,30] The reaction presumably proceeds via cleavage of the carbonic acid dimethyl ester which leads to the intermediate dithiolate which subsequently reacts with electrophilic alkylhalogen to afford the 3,4-disubstituted pyrrole rings.

On the other hand, the detosylation reaction was also performed in the presence of sodium methoxide.[28] In our case, the reactivity of the dithiolone functional group toward sodium methoxide was found to be higher than the detosylation reaction. Actually, the intermediate *N*-protected 3,4-methylenedithiopyrrole was successfully isolated, and the structure was confirmed by the ^{1}H NMR and EI-mass spectra.[26] Further treatment with sodium methoxide gave the desired 3,4-alkylenedithiopyrroles by deprotection of the tosyl group. However, a one-pot reaction leading to 3,4-alkylenedithiopyrroles could also be performed by addition of a large excess of sodium methoxide and at longer reaction time. Although a higher temperature was found to accelerate the reaction, it did result in a lower yield due to the increasing formation of byproducts.

Direct alkylation of dithiol−thione compounds has also been reported by Kanatzidis et al.;[31] however, they used stronger potassium methoxide and higher temperature (50 °C), which suggests that dithiol−thione compounds possess a lower reactivity than dithiolones. This was further clearly confirmed by the selective alkylation of the dithiolone of 6-thioxo-1,3,5,7-tetrathia-*s*-indecen-2-one, where the two different groups, dithiolone and dithiol−thione, were both present in one molecule.[30] However, detosylation of **3** has also been reported in the presence of sodium methoxide affording (1,3)-dithiolo[4,5-*c*]pyrrol-2-thione, although increasing reaction temperature made the alkylation of dithiol−thione possible, too.[28] The reaction suggested the higher reactivity of detosylation compared to alkylation of the dithiol−thione group. On the basis of the above discussion, the reactivity sequence of functional groups appears to be dithiolone > tosyl > dithiol−thione. Since the alkylation of deprotected pyrrole (NH) is a potentially competitive reaction of alkylation of dithiol−thione, it is reasonable to transchalcogenate **3** to **4**, which can first be alkylated and then deprotected to afford the desired 3,4-alkylenedithiopyrroles. The proposed structures of the 3,4-disubstituted pyrroles were confirmed by ^{1}H NMR, ^{13}C NMR and MS spectra.

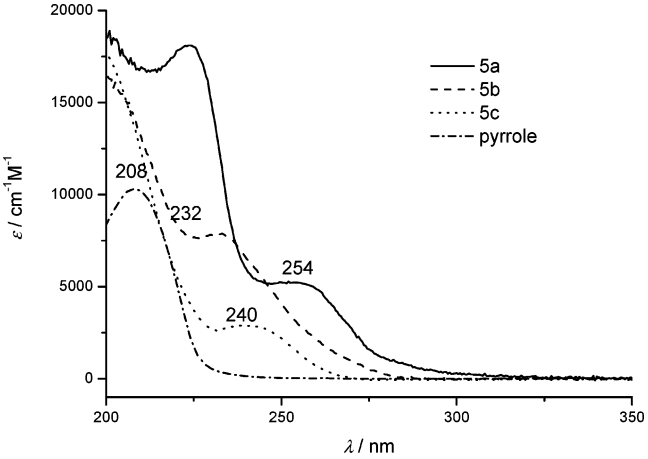

Figure 1. UV−vis absorption spectra of monomers **5a**−**c** in cyclohexane.

Table 1. Optical and Electrochemical Data for the 3,4-Disubstituted Pyrroles

monomer	λ_{max} (nm)	λ_{onset} (nm)	E_{opt} (eV)[a]	$E_{ox,p}$ (V)	$E_{ox,onset}$ (V)
5a	254	∼310	4.00	0.60	0.50
5b	232	∼280	4.44	0.58	0.45
5c	240	263	4.71	0.71	0.61
pyrrole	208	227	5.46	1.00	0.77

[a] The optical energy gap estimated from the onset absorption of monomer solution in cyclohexane.

UV—Vis Absorption Properties and Electrochemistry of the 3,4-Disubstituted Pyrroles. The UV−vis absorption spectra of the 3,4-disubstituted pyrroles **5a**−**c** were recorded in dilute solutions (about 10^{-5} M) in cyclohexane (Figure 1). For comparison, the absorption of pyrrole was also recorded under the same conditions. As shown in Figure 1, **5a** displays its absorption maximum at 254 nm. The true onset absorption is difficult to determine because of the long absorption tail that extends far beyond 300 nm. However, we estimate the onset to be at ca. 310 nm. Compared with **5a**, 3,4-ethylenedithiopyrrole (**5b**) shows its absorption peaking at shorter wavelength (232 nm), the corresponding onset absorption blue-shifts to ca. 280 nm. The absorption maximum of **5c** peaks at 240 nm, which is intermediate between those of **5a** and **5b**. However, **5c** possesses the highest onset absorption energy (263 nm) and, consequently, the highest optical energy gap (4.71 eV). Compared with that of parent pyrrole, the absorptions of **5a**−**c** are red-shifted which shows that the electron donating alkylthio substituents at β positions generally lower the optical lowest-energy transition of the 3,4-disubstituted pyrroles. The detailed optical data are listed in Table 1. Time dependent DFT computations at B3LYP/6-31+G**//B3LYP/6-31G* level of theory[32] show that the four longest-wavelength absorptions of **5a**,**b** are HOMO(−1) → LUMO(+1) transitions (λ_{max} = 327, 298, 270, and 259 nm for **5a** and 281, 280, 272, and 269 nm for **5b**). While the HOMO(−1) are π orbitals, the LUMO(+1) are σ orbitals. Thus, for symmetry reasons, these transitions are weak but will gain intensity the more the sulfur substituents are twisted out of the σ plane. This is clearly the case for **5a** where the DFT

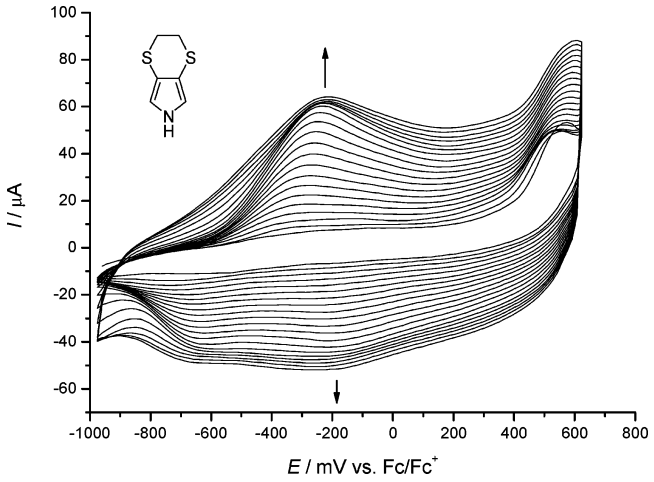

Figure 2. Cyclic voltammogram of **5b** in TBAH-ACN.

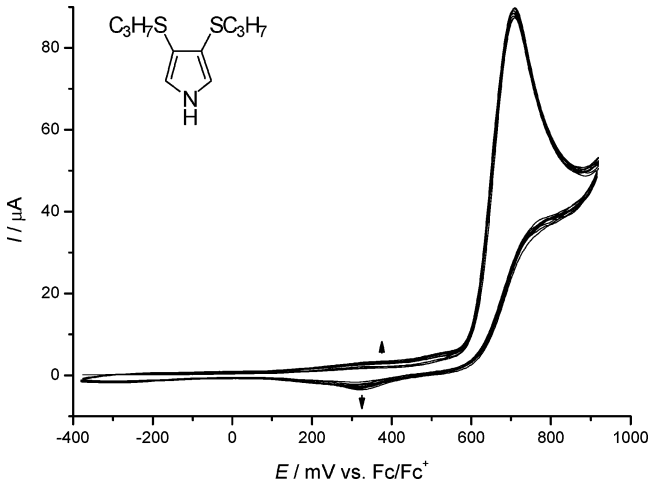

Figure 3. Cyclic voltammogram of **5c** in TBAH-ACN.

optimizations yield an envelop structure for the methylenedithio five-membered ring, as well as for **5b** where the ethylenedithio six-membered ring adopts a twist structure. Thus, steric factors govern the intensity of the lowest-energy $\pi \rightarrow \sigma^*$ transitions of **5a**−**c**.

Cyclic voltammetry (CV) investigations of **5a**−**c** were carried out in dry acetonitrile (ACN) using tetrabutylammonium hexafluorophosphate (Bu_4NPF_6, TBAH) as the supporting electrolyte. All the 3,4-disubstituted pyrroles **5a**−**c** possess an irreversible oxidation behavior over the potential range of 0.57−0.71 V (vs Fc/Fc^+) (see the corresponding first CV scans in Figures 2 and 3). The observed oxidation potentials of **5a**−**c** are lower than those of parent pyrrole (1.00 V vs Fc/Fc^+) and the other analogues, such as 3,4-ethylenedioxypyrrole (EDOPy) (0.73 V vs Fc/Fc^+)[25] and those reported for EDOT and EDTT.[33] The low oxidation potential of monomers **5a**−**c** is due to the strong electron donating dialkylthio substituents at the 3- and 4-positions of pyrrole and suggests advantageous electropolymerization properties. A lower electropolymerization potential of pyrroles is desirable in order to prevent overoxidation of resulting polypyrroles since bond formation and doping of the polymers generally proceed simultaneouly.[34]

3,4-Ethylenedithiopyrrole **5b** displays a similar potentiodynamic electropolymerization behavior as 3,4-methylenedithiopyrrole **5a**.[26] Figure 2 shows the fast formation of poly(**5b**) film on the platinum working electrode. Much in contrast, the corresponding potentiodynamic cycling of **5c** with two propylthio side chains at β positions exhibits a quite slow

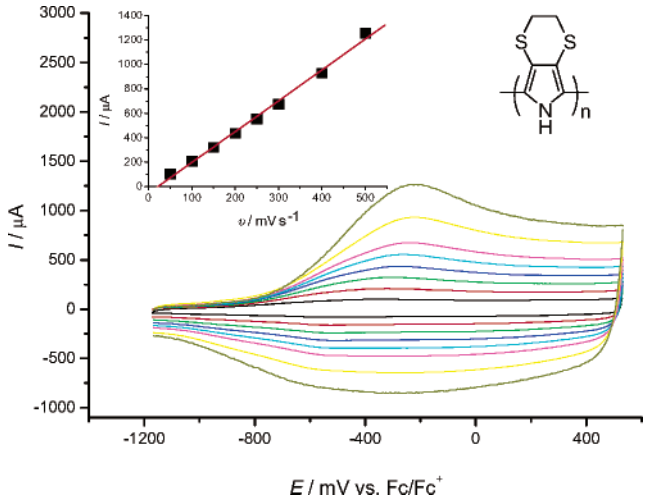

Figure 4. Cyclic voltammogram of poly(**5b**) in TBAH-ACN.

polymer growth on the electrode surface (Figure 3). This might be due to the better solubility of poly(**5c**) owing to the attached alkylthio side chains. For a better comparison the optical and electrochemical properties of **5a**−**c**, the detailed absorption and electrochemical data including the calculated optical energy gap are listed in Table 1.

Monomer Polymerization and Electrochemistry of Polymers. Repetitive potential scans (over the potential range of −1.00 to +0.80 V vs Fc/Fc^+) applied to solutions of monomers **5a**−**c** in ACN results in a new redox process with lower potential than the monomer oxidation potential (Figures 2 and 3). The current intensity of the new redox process increases with repeating scans indicating conducting polypyrrole deposition on the electrode surface. These polymers are visible as yellow deposits on the electrode surface. After the polymer-deposited electrode has been washed with the monomer free electrolyte for several times the CVs of the resulting polymers were measured in monomer free electrolyte. Figure 4 shows the reversible CVs of poly(**5b**) at different scan rates (from 50 to 500 mV s^{-1}). The much lower redox potential of poly(**5b**) with oxidation peaks at −0.22 V (vs Fc/Fc^+) compared to that of previously reported poly(**5a**) ($E_{ox,p}$ = 0.17 V) demonstrates that the side chains attached at 3- and 4-positions play an even more important role for the properties of the polymers than for that of the monomers given the fact that the oxidation potentials of corresponding monomers are almost identical. The inset of Figure 4 shows that the current intensity of the redox process of the resulting polymer is proportional to the scan rates over the range 50−500 mV s^{-1}. This indicates that the polymer is confined to the electrode and the redox process is reversible.

Besides the potentiodynamic polymerization, the corresponding conjugated poly(3,4-disubstituted-pyrrole)s could also be prepared by bulk electrolysis of monomers **5a**−**c** at a little higher potential than their corresponding oxidation peaks (0.03 V + $E_{ox,p}$)[34] or by galvanostatic method at low current levels. Figure 5 displays the CV of poly(**5c**) which was polymerized on the electrode by holding the working electrode potential at 0.74 V (vs Fc/Fc^+) for 10 min. The corresponding redox process of poly(**5c**) shows an oxidation peak at 0.46 V, which corresponds to the Faradaic p-doping of the polymer to afford conducting oxidized polymer. Unfortunately, efforts to obtain the corresponding free-standing polymer films failed due to the fragility of the resulting films.

By chemical oxidative polymerization of **5a** in ACN using $FeCl_3$ as a convenient oxidant, poly(**5a**) was also successfully prepared as purplish black powder.

Table 2. Optical and Electrochemical Data for Poly(pyrrole)s

polymer	$h\nu_{max}$ (eV) (slightly oxidized)	$h\nu_{max}$ (eV) (oxidized)	$E_{ox,pa}$ (V)	$E_{ox,pc}$ (V)	$\Delta E_{ox,pc}$ (V)	$E_{ox,onset}$ (V)	HOMO (eV)[a]	band gap (eV)[b]
poly(**5a**)	2.58, 1.06	2.79, 0.97	0.17	0.07	0.10	−0.33	−4.47	1.8
poly(**5b**)	2.57, 1.74, 1.19, 0.68	3.14, 1.91, 0.95	−0.22	−0.28	0.06	−0.70	−4.10	2.1
poly(**5c**)	3.00, 2.81, 2.62	2.82, 2.62, 2.20, 2.02, 0.79	0.46	0.34	0.12	0.15	−4.95	2.3
PPy	3.2, 2.1, 1.4, 0.7	3.6, 2.7, 1.0	0.12	−0.07	0.19	−0.35	−4.45	2.8

[a] The HOMO level is calculated from the onset potential of oxidation (vs. Fc/Fc^+) according to the empirical equation $E^{HOMO} = -e(E_{onset} + 4.8)$ V by assuming the energy level of Fc/Fc^+ to be −4.8 eV below the vacuum level. [b] From the onset of the absorption spectra.

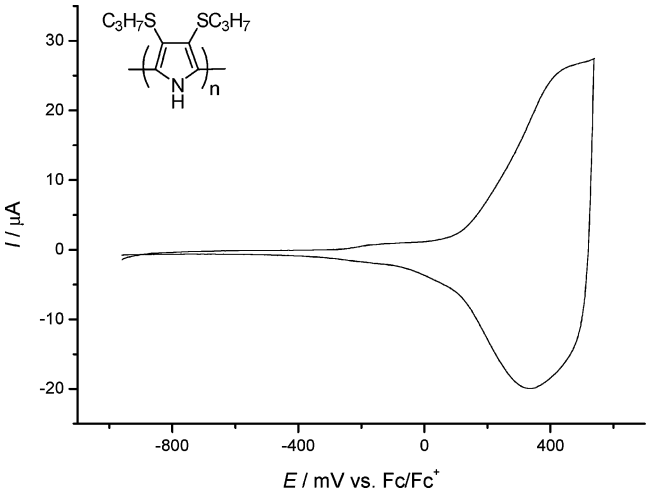

Figure 5. Cyclic voltammogram of poly(**5c**) in TBAH-ACN.

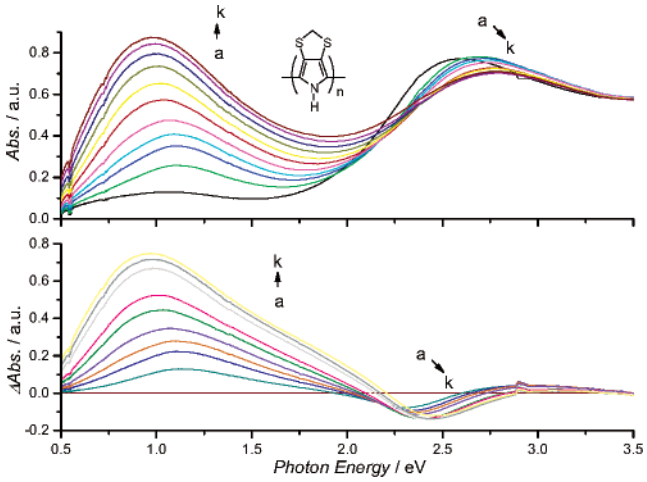

Figure 6. Spectroelectrochemistry (upper figure) and difference spectra between highly oxidized state and initial slightly oxidized state of poly(**5a**) (lower). Key: (a) −1.0 V; (b−k) 0.2−1.0 V, step 0.1 V; vs Fc/Fc^+.

For a better comparison the electrochemical properties of the corresponding polymers, the onset of oxidation of the polymers are given in Table 2. From these data we calculated the HOMO energy level by applying the empirical equation $E^{HOMO} = -e(E_{onset} + 4.8)$V.

UV—Vis—NIR Absorption Properties and Spectroelectrochemistry of Polymers. The UV−vis−NIR absorption and spectroelectrochemistry (SEC) studies of the polymers were performed with electropolymerized polymer films on a polished Pt electrode in reflection mode.[35] The spectrum of slightly oxidized poly(**5a**) (which we could not fully reduce even at very negative potential) is featured by a strong absorption at 2.58 eV, which is assigned to the interband transition of the undoped polymer (see Figure 6). In the lower energy region, there is a weak but very broad absorption which is due to slightly doped polymer. At a much high oxidation state, poly(**5a**) possesses a very strong and broad absorption peak at 0.97 eV, and the corresponding band gap transition shifts to 2.79 eV. The broad and featureless low-energy absorption gives only poor information about the electronic structure of poly(**5a**). However, the difference spectra between that of a highly oxidized states and that of slightly doped poly(**5a**) suggests a shoulder at about 1.70 eV. Comparison with the spectra of polypyrrole[36] indicates that bipolaron charges are formed in poly(**5a**), at least at the higher oxidized states. On the other hand, given the fact that the CV of poly(**5a**) shows a pronounced Faradaic charging behavior (almost symmetrical anodic and cathodic redox waves) typical of redox polymers, the strong and featureless absorption at 0.97 eV might be interpreted as intervalence charge-transfer bands.[37]

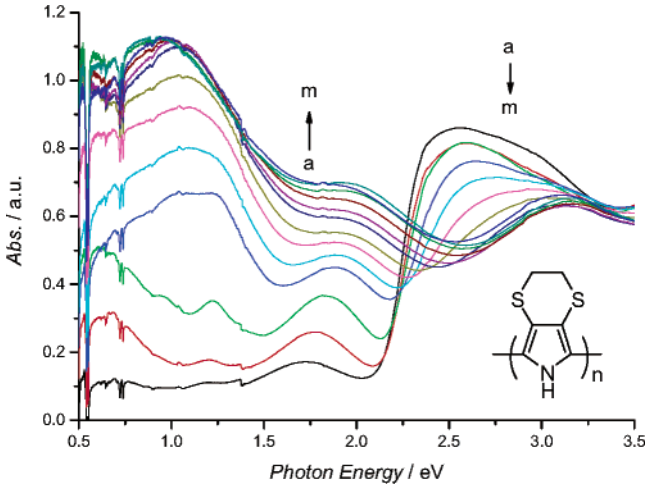

Figure 7. Spectroelectrochemistry of poly(**5b**) on Pt: (a−k) −0.9−0.1 V, step 0.1 V; (l) 0.3 V; (m) 0.6 V vs Fc/Fc^+.

Much in contrast poly(**5b**) and poly(**5c**) display a more pronounced spectroelectrochemistry. In comparison with the absorption of poly(**5a**), poly(**5b**) shows a similar strong absorption peak at 2.57 eV (Figure 7). However, there are three much weaker absorptions in the lower energy region (0.68, 1.19, and 1.74 eV) even at very negative potential. These features are in agreement with the optical spectrum reported for polypyrrole.[36] The maximum absorption at 2.57 eV can be assigned to the interband transition. The other three additional absorptions are due to the corresponding transitions within the gap region: the 1.19 eV absorption suggests that poly(**5b**) forms a polaron upon weak oxidation; this band is associated with the transition from the bonding to the antibonding polaron state. The absorption at 0.68 eV is believed to be due to the transition from the valence band (VB) to the bonding polaron state; the peak at 1.74 eV might originate from the transition from the VB to the antibonding polaron state. Along with the increase of doping level, the polaron transition disappears, and three strong absorption peaks characterize the highly oxidized polymer: the band gap transition at 3.14 eV is 0.57 eV larger than that of slightly doped state, and the transitions at 0.95 and 1.91 eV are assigned to the bipolaron transitions at the highly doped state.

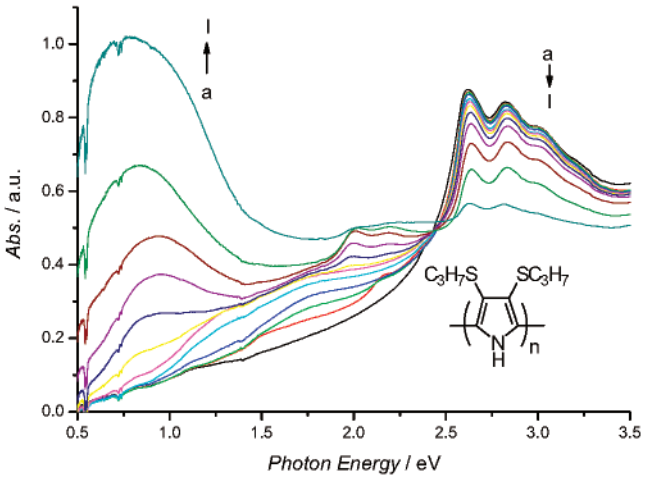

Figure 8. Spectroelectrochemistry of poly(**5c**) on Pt: (a) −0.9 V; (b) −0.7 V; (c) −0.4 V; (d−l) −0.2−0.7 V step: 0.1 V; vs Fc/Fc^+.

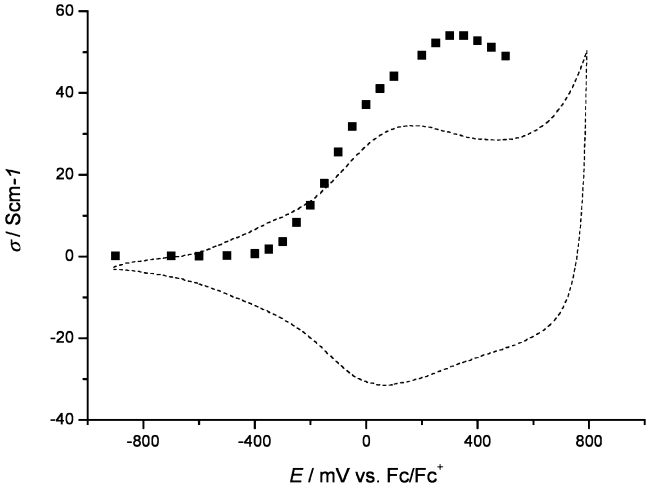

Figure 9. In situ conductivity vs potential for poly(**5a**). Dashed curve: CV for comparison.

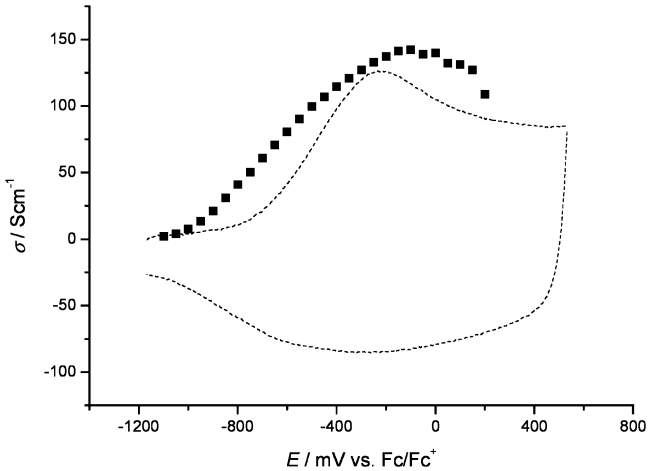

Figure 10. In situ conductivity vs potential for poly(**5b**). Dashed curve: CV for comparison.

As shown in Figure 8, poly(**5c**) possesses a significantly more fine-structured absorption over the range of 2.62 eV to 3.00 eV, indicating a higher degree of regularity in poly(**5c**) compared to poly(**5a**) and poly(**5b**). This is possibly due to steric effects of the longer and bulkier side chains. The long tail in the low energy region of the spectra indicates the slightly oxidized state of poly(**5c**). This extended tail of absorption makes the determination of transitions within the gap region more difficult. However, at highly doped state, besides the band gap absorption at 2.62 eV, the strong absorption peaks at 0.79 and 2.0−2.2 eV suggest a bipolaron state of poly(**5c**).

The bathochromic shift of the band gap absorptions of poly(**5a**)−poly(**5c**) (2.5−3.0 eV) compared with that of parent polypyrrole (3.30 eV) is expected due to the auxochromic effect of the electron donating alkylthio subsituents at the 3- and 4-positions of pyrrole ring. It has to be noted that the polymers prepared by electrochemical oxidation polymerization are difficult to fully reduce to their neutral states, possibly due to the effect of hampered counteranion diffusion. The coexisting absorption peaks of the slightly oxidized states and extension of the absorption tails make the determination of the optical band gap of neutral polymers deduced from the onset of absorption difficult. Approximate onset values are given in Table 2.

Poly(**5a**) possesses the smallest band gap of 1.8 eV among the three polypyrroles. The higher optical band gaps of neutral poly(**5b**) and poly(**5c**) are determined to be 2.1 and 2.3 eV, respectively. The increase of band gap might be rationalized on a steric basis, i.e., different biaryl torsional angles induced by the different size of the alkylthio substituents, and/or different conformations that alkylthio substituents adopt (the six-membered ring of EDTPy dimer was reported to adopt a twist conformation[38]). On the other hand, the polypyrroles show a similar trend of band gap as the optical energy gap of the monomers which indicates that the polypyrrole band gap is mainly governed by electronic effects already present in the monomers as discussed above. These polymer band gaps are comparable to those of analogous poly(3,4-alkylenedioxy)-pyrroles (2.1−2.2 eV), but are of course much lower than the values reported for PPy (2.8 eV).[39] Not only the electron-donating substituents, but also the potential formation of an intramolecular hydrogen bond[38] between the N−H group of a given pyrrole ring and the closest S atom of the neighboring rings that stabilized the planar anti conformation might contribute to the decrease of band gap of the substituted polypyrroles. This demonstrates that polymers based on alkylthiopyrroles are well suited to tune the electronic properties of polypyrroles.

In Situ Conductivity of the Polymers. In situ conductivity measurements using a two-band electrode show that the poly(**5a**)−poly(**5c**) can be switched between a neutral nonconductive and an oxidized conductive state by controlling the oxidation potential.

Figure 9 shows the in situ conductivity of poly(**5a**) depending on the oxidation potentials. The oxidation leads to the transition from a neutral low-conductive state to a highly conductive state. After passing a maximum (54 S cm^{-1}), the conductivity of poly(**5a**) decreases along with a further increase of oxidation potential, probably due to the overoxidation of poly(**5a**) The maximum of conductivity is slightly above the maximum Faradaic charging potential. As the spectroelectrochemistry of the polymers suggests, the bipolarons dominate the electronic structure of poly(**5a**−**c**) at the highly doped levels. According to the 3D-hopping transport model of bipolaron charges, both bipolaron-carrying and bipolaron-free polymer segments are required for electronic conduction. When the required bipolaron-free segments are also oxidized (overoxidation) at higher potentials, the transfer of bipolaron charges to bipolaron-free moieties decreased, and this accounts for the decrease of conductivity along further oxidation after passing a maximum.[40] The observed sigmoid shape of conductivity vs potential has also been reported for other polypyrroles.[41]

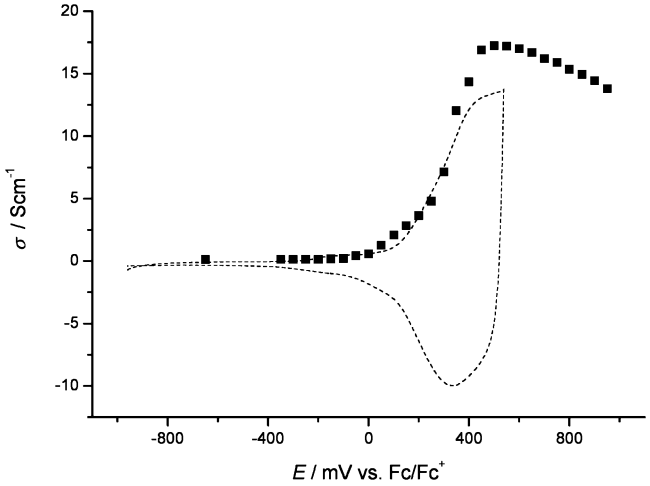

Figure 11. In situ conductivity vs potential for poly(**5c**). Dashed curve: CV for comparison.

Figures 10 and 11 depict analogous sigmoid curves of in situ conductivity vs potentials for poly(**5b**) and poly(**5c**), respectively. The corresponding maximum conductivity is found to be 142 S cm^{-1} for poly(**5b**) at −0.16 V and 17 S cm^{-1} for poly(**5c**) at 0.5 V. Under the same experimental conditions the maximum conductivity of polypyrrole was measured to be 271 S cm^{-1} at 0.2 V.

Although our conductivity measurements are only semiquantitative it is clear that at least poly(**5b**) has a conductivity of similar magnitude as parent polypyrrole.

Conclusions

In summary, three 3,4-bis(alkylthio)pyrroles (**5a**−**c**) were prepared and the corresponding conducting polymers were successfully synthesized by anodic electropolymerization and/or chemical oxidation using $FeCl_3$ as oxidant. The monomers possess significantly lower oxidation potentials than unsubstituted pyrrole due to the substitutions of electron donating alkylthio groups at 3- and 4-positions. UV−vis−NIR absorption and spectroelectrochemistry investigations of polypyrroles suggest that the optical band gaps are much lower than that of unsubstituted pyrrole, and similar to those of the analogous poly(3,4-alkylenedioxy)pyrroles. Bipolaron charges are formed in all three polymers at the highly doped states. The in situ conductivity measurements show that the polymers can be switched between a neutral nonconductive and an oxidized conductive state. In contrast to poly(3,4-alkylenedioxy)pyrroles, the dithiopyrroles show much higher in situ conductivities comparable to that of polypyrrole.

Acknowledgment. H.L. thanks the Alexander von Humboldt Foundation for financial support.

References and Notes

(1) Meanwell, N. A.; Romine, J. L.; Rosenfeld, M. J.; Martin, S. W.; Trehan, A. K.; Wright, J. J. K.; Malley, M. F.; Gougoutas, J. Z.; Brassard, C. L.; Buchanan, J. O.; Federici, M. E.; Fleming, J. S.; Gamberdalla, M.; Hartl, K. S.; Zavoico, G. B.; Seiler, S. M. *J. Med. Chem.* **1993**, *36*, 3884.
(2) Franck, B.; Nonn, A. *Angew. Chem., Int. Ed. Engl.* **1995**, *34*, 1795.
(3) Banwell, M. G.; Flynn, B. L.; Hamel, E.; Hockless, D. C. R. *Chem. Commun.* **1997**, 207.
(4) Haddour,; Cosnier, N. S.; Gondran, C. *Chem. Commun.* **2004**, 2472.
(5) Zong, K.; Abboud, K. A.; Reynolds, J. R. *Tetrahedron Lett.* **2004**, *45*, 4973.
(6) Thomas, C. A.; Zong, K.; Schottland, P.; Reynolds, J. R. *Adv. Mater.* **2000**, *12*, 222.
(7) Guernion, N. J. L.; Hayes, W. *Curr. Org. Chem.* **2004**, *8*, 637.
(8) Smela, E. *Adv. Mater.* **2003**, *15*, 481.
(9) Zotti, G.; Zecchin, S.; Schiavon, G.; Vercelli, B.; Berlin, A.; Grimoldi, S. *Macromol. Chem. Phys.* **2004**, *205*, 2026.
(10) Diaz, A. F.; Castillo, J. I.; Logan, J. A.; Lee, W. Y. J. *J. Electroanal. Chem.* **1981**, *129*, 115.
(11) Anderson, H. J.; Loader, C. E.; Xue, R. X.; Lê, N.; Gogan, N. J.; McDonald, R.; Edwards, L. G. *Can. J. Chem.* **1985**, *63*, 896.
(12) Shiraishi, H.; Nishitani, T.; Nishihara, T.; Sakaguchi, S.; Ishii, Y. *Tetrahedron* **1999**, *55*, 13957.
(13) Liu, J.-H.; Chan, H.-W.; Wong, H. N. C. *J. Org. Chem.* **2000**, *65*, 3274.
(14) Phadmavathi, V.; Jagan Mohan Reddy, B.; Sarma, M. R.; Thriveni, P. *J. Chem. Res.* **2004**, *2004*, 79.
(15) Airaksinen, A. J.; Ahlgren, M.; Vepsäläinen, J. *J. Org. Chem.* **2002**, *67*, 5019.
(16) Shum, P. W.; Kozikowski, A. P. *Tetrahedron Lett.* **1990**, *31*, 6785.
(17) Groves, J. K.; Cundasawmy, N. E.; Aderson, H. J. *Can. J. Chem.* **1973**, *51*, 1089.
(18) Kaminovz, Y.; Smela, E.; Johansson, T.; Brehmer, L.; Anderson, M. R.; Ingänas, O. *Synth. Met.* **2000**, *113*, 103.
(19) Argun, A. A.; Aubert, P.-H.; Thompson, B. C.; Schwendeman, I.; Gaupp, C. L.; Hwang, J.; Pinto, N. J.; Tanner, D. B.; MacDiarmid, A. G.; Reynolds, J. R. *Chem. Mater.* **2004**, *16*, 4401.
(20) Bao, Z.; Lovinger, A. J. *Chem. Mater.* **1999**, *11*, 2607.
(21) Saricftci, N. S. *Mater. Today* **2004**, *7*, 36.
(22) Roncali, J.; Blanchard, P.; Frère, P. *J. Mater. Chem.* **2005**, *15*, 1589.
(23) Turbiez, M.; Frère, P.; Allain, M.; Gallego-Planas, N.; Roncali, J. *Macromolecules* **2005**, *38*, 6808.
(24) Mas-Torrent, M.; Murkut, M.; Hadley, P.; Ribas, X.; Rovira, C. *J. Am. Chem. Soc.* **2004**, *126*, 984.
(25) Groenendaal, L.; Zotti, G.; Aubert, P.-H.; Waybright, S. M.; Reynolds, J. R. *Adv. Mater.* **2003**, *15*, 855.
(26) Li, H.; Lambert, C. *J. Mater. Chem.* **2005**, *15*, 1235.
(27) Schiavon, G.; Sitran, S.; Zotti, G. *Synth. Met.* **1989**, *32*, 209.
(28) Jeppesen, J. O.; Takimiya, K.; Jensen, F.; Brimert, T.; Nielsen, K.; Thorup, N.; Becher, J. *J. Org. Chem.* **2000**, *65*, 5794.
(29) Frère, P.; Gallego-Planas, N.; Blanchard, P.; Mabon, G.; Rondeau, D. *Tetrahedron Lett.* **2002**, *43*, 1825.
(30) Larsen, J.; Bechgaard, K. *J. Org. Chem.* **1987**, *52*, 3285.
(31) Wang, C.; Schindler, J. L.; Kannewurf, C. R.; Kanatzidis, M. G. *Chem. Mater.* **1995**, *7*, 58.
(32) Gaussian 03. Gaussian 03, Revision B.04. Frisch, M. J.; Trucks, G. W.; Schlegel, H. B.; Scuseria, G. E.; Robb, M. A.; Cheeseman, J. R.; Montgomery, J. A.; Vreven, Jr., T.; Kudin, K. N.; Burant, J. C.; Millam, J. M.; Iyengar, S. S.; Tomasi, J.; Barone, V.; Mennucci, B.; Cossi, M.; Scalmani, G.; Rega, N.; Petersson, G. A.; Nakatsuji, H.; Hada, M.; Ehara, M.; Toyota, K.; Fukuda, R.; Hasegawa, J.; Ishida, M.; Nakajima, T.; Honda, Y.; Kitao, O.; Nakai, H.; Klene, M.; Li, X.; Knox, J. E.; Hratchian, H. P.; Cross, J. B.; Adamo, C.; Jaramillo, J.; Gomperts, R.; Stratmann, R. E.; Yazyev, O.; Austin, A. J.; Cammi, R.; Pomelli, C.; Ochterski, J. W.; Ayala, P. Y.; Morokuma, K.; Voth, G. A.; Salvador, P.; Dannenberg, J. J.; Zakrzewski, V. G.; Dapprich, S.; Daniels, A. D.; Strain, M. C.; Farkas, O.; Malick, D. K.; Rabuck, A. D.; Raghavachari, K.; Foresman, J. B.; Ortiz, J. V.; Cui, Q.; Baboul, A. G.; Clifford, S.; Cioslowski, J.; Stefanov, B. B.; Liu, G.; Liashenko, A.; Piskorz, P.; Komaromi, I.; Martin, R. L.; Fox, D. J.; Keith, T.; Al-Laham, M. A.; Peng, C. Y.; Nanayakkara, A.; Challacombe, M.; Gill, P. M. W.; Johnson, B.; Chen, W.; Wong, M. W.; Gonzalez, C.; Pople, J. A. Gaussian, Inc.: Pittsburgh, PA, 2003.
(33) Blanchard, P.; Cappon, A.; Levillain, E.; Nicolas, Y.; Frère, P.; Roncali, J. *Org. Lett.* **2002**, *4*, 607.
(34) Sadki, S.; Schottland, P.; Brodie, N.; Sabouraud, G. *Chem. Soc. Rev.* **2000**, *29*, 284.
(35) Salbeck, J. *J. Electroanal. Chem.* **1992**, *340*, 169.
(36) Brédas, J. L.; Scott, J. C.; Yakushi, K.; Street, G. B. *Phys. Rev. B* **1984**, *30*, 1023.
(37) Lambert, C.; Nöll, G. *Synth. Met.* **2003**, *139*, 57.
(38) Alemán, C.; Casanovas, J. *J. Phys. Chem. A* **2004**, *108*, 1440.
(39) Sönmez, G.; Schottland, P.; Zong, K.; Reynolds, J. R. *J. Mater. Chem.* **2001**, *11*, 289.
(40) Chance, R. R.; Brédas, J. L.; Silbey, R. *Phys. Rev. B* **1984**, *29*, 4491.
(41) Zotti, G.; Zecchin, S.; Schiavon, G.; Vercelli, B.; Berlin, A.; Dalcanale, E.; Groenendaal, L. *Chem. Mater.* **2003**, *15*, 4642.

MA0601868